Adaptive Beam Director for a Tiled Fiber Array

Mikhail A. Vorontsov
Intelligent Optics Laboratory, Computational and Information Sciences Directorate, U.S. Army Research Laboratory, 2800 Powder Mill Road, Adelphi, Maryland 20783 and Intelligent Optics Laboratory, Institute for Systems Research, University of Maryland, 2107 Technology Ventures Building, College Park, Maryland 20742; e-mail: mvorontsov@arl.army.mil

Jim F. Riker
AFRL/DESM, Air Force Research Laboratory, 535 Lipoa Parkway, suite 200, Kiehei, HI 96753; e-mail: Jim.Riker@maui.afmc.af.mil

Ernst Polnau
Intelligent Optics Laboratory, Institute for Systems Research, University of Maryland, 2107 Technology Ventures Building, College Park, Maryland 20742; e-mail: epolnau@mail.umd.edu

Svetlana L. Lachinova
Intelligent Optics Laboratory, Institute for Systems Research, University of Maryland, 2107 Technology Ventures Building, College Park, Maryland 20742; e-mail: sllachin@mail.umd.edu

V. S. Rao Gudimetla
AFRL/DESM, Air Force Research Laboratory, 535 Lipoa Parkway, suite 200, Kiehei, HI 96753; e-mail: Rao.Gudimetla@maui.afmc.af.mil

Abstract

We present the concept development of a novel atmospheric compensation system based on adaptive tiled fiber array architecture operating with target-in-the-loop scenarios for directed beam applications. The adaptive tiled fiber array system is integrated with adaptive beam director (ABD). Wavefront control and sensing functions are performed directly on the beam director telescope primary mirror. The beam control of the adaptive tiled fiber array aims to compensate atmospheric turbulence-induced dynamic phase aberrations and results in a corresponding brightness increase on the illuminated extended object. The system is specifically designed for tiled fiber system architectures operating in strong intensity scintillation and speckle-modulation conditions typical for laser-illuminated extended objects and includes both local (on-tile) wavefront distortion compensation and phase locking of sub-systems. The compensation algorithms are based on adaptive optimization of performance metrics. Local wavefront distortion compensation is performed using on-tile stochastic parallel gradient descent (SPGD) optimization of local speckle metrics directly measured on each fiber-tile. Phase locking is performed using SPGD optimization of a composed metric, that is, the metric combined from the local metrics. An experimental setup is developed to evaluate the feasibility of controlling beam quality by using speckle metrics based on the temporal analysis of the speckle pattern of light which is backscattered from a laser-illuminated extended object and recorded by a single photo-detector. The experimental setup is used to investigate beam quality improvement, adaptive process convergence, and the influence of the illuminated object shape.

1. Introduction

It is now well understood that further development of existing large-aperture beam forming telescopes will lead to a heavy and bulky expensive assembly composed of monolithic primary and secondary mirrors. The shortcomings of large-aperture monolithic systems stimulated the recent development of beam director systems composed of a phase-locked (coherent) array of small densely packed laser transmitter telescopes (sub-systems), referred to as conformal optical systems. Indeed, the conformal beam forming assembly can be more compact, significantly less expensive, and lighter. Moreover, the conformal architecture is scalable and robust to element failure. The increasing interest in phase-locked conformal optical systems has recently stimulated significant growth of phase-locking techniques. Nevertheless, the development of optical conformal beam forming systems performing in the presence of atmospheric turbulence represents a very challenging problem. In fact, it can be shown that tiled fiber arrays under atmospheric conditions with relatively small Fried parameters r0 require several thousands highly accurate aligned fiber-tiles for full compensation of atmospheric effects if only a piston control (phase-locking) is used. One of the major problems resulting from the complicated architecture is that the entire system is highly vulnerable to environmental influences. For example, vibrations, high accelerations, and also high-thermal gradients are problematic for such systems. This leads to a strong interest in new robust adaptive beam control capabilities.

In this paper we introduce a new concept, referred to as *Adaptive Beam Director* (ABD). The ABD system consists of a beam forming telescope with wavefront compensation integrated solely on its primary mirror. This new system is capable of operating in strong-scintillation conditions with both unresolved (point-source) and resolved (extended) objects towards which the beam is directed. The ABD system can either be combined with phase-locked tiled fiber array systems to improve their stability against environmental influences or it can be implemented in conventional beam directors with the monolithic aperture to achieve a robust beam forming capability.

The new ABD control system introduces additional wavefront compensation degrees of freedom besides the piston control into a phase-locked tiled fiber array system. This introduction has several advantages. Firstly, it allows us to achieve good system performance with smaller number (100 or less) of installed and mutually aligned fiber-tiles. Secondly, these additional degrees of freedom make possible the compensation of fiber-tile misalignments caused by dynamically changing thermal expansion and vibrations within the system. This makes the whole system more robust to environmental influences.

In this new concept the control of the on-mirror adaptive optics can be performed using the stochastic parallel gradient descent (SPGD) algorithm. The SPGD algorithm is designed for laser beam control systems in which reflected from an illuminated object light is used for SPGD performance metric measurements. These metrics act as quality parameters, providing information about the size of the laser hot spot on the object. Depending on the application scenario and/or the object type, different types of metrics can be considered in the ABD system. In this work we mostly concentrate on the time-varying speckle metrics which are based on temporal fluctuations of the speckle field reflected from the extended laser-illuminated objects. In particular, we investigate a sensitivity of these metrics to the laser beam intensity concentration on the extended object surfaces and further compare it to the sensitivity of the so-called power-in-the-bucket (PIB) metrics, typically associated with unresolved object scenarios.

2. ABD control system

2.1. Design of ABD system

Fig.1 illustrates the new on-mirror adaptive beam director concept. The ABD works basically as a telescope, consisting of a primary mirror and a secondary mirror. This primary mirror is a key component of the ABD telescope. It contains an array of pockets machined on its backside and is therefore also called a pocket-mirror. Within these pockets sensor lenslets with photo-detector arrays, the SPGD controllers, on-chip amplifiers, and piezo-electrical components are placed (see Fig.2). The piezo-electrical component consists of electrically sectioned piezo-ceramic annular rings made from thin (~0.3mm) bimorph discs glued to the pocket bottom. By applying a voltage to the electrodes of the elements, the curvature of the local front (mirror) surface opposite to the pocket bottom can be changed.

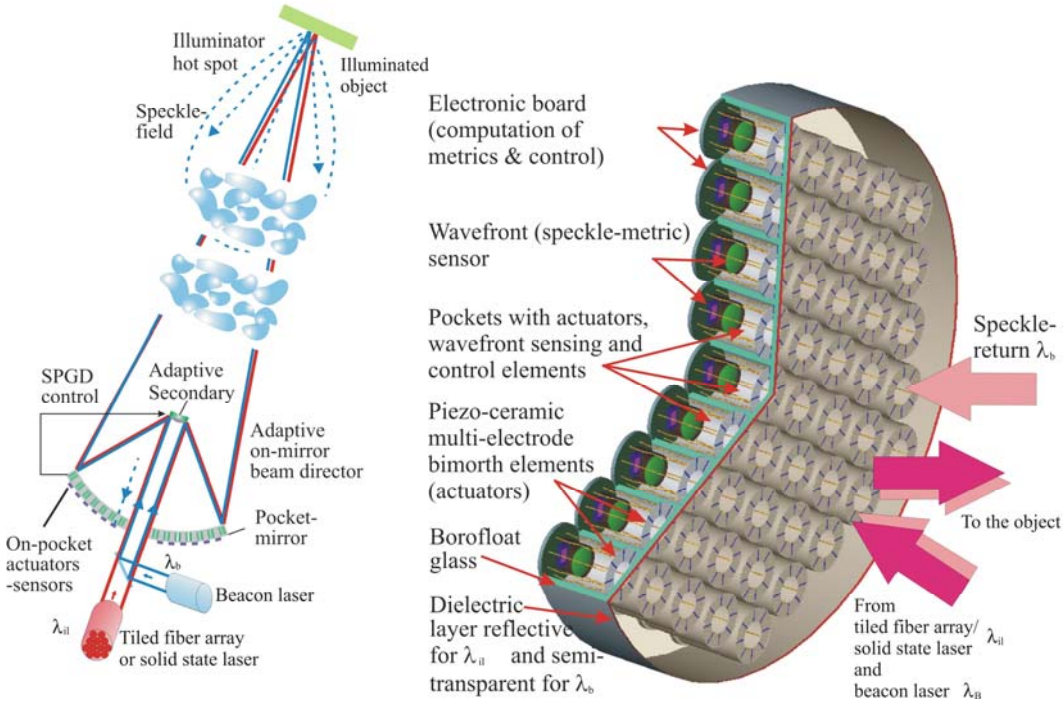

Fig.1. Adaptive beam director concept using either phase-locked tiled fiber array or a solid-state high energy laser as input (left). On-pocket mirror with integrated wavefront sensing and control sub-systems (right).

On the front surface of the pocket-mirror a special dielectric layer is deposited which is highly reflective for one wavelength λ_{il} and semi-transparent for a slightly different wavelength λ_b. This enables the system to work with two different laser beams at these wavelengths. The source of radiation with wavelength λ_{il} can either be a solid state laser source or the output from a tiled fiber array. This beam is combined with a second beam λ_b by a beam splitter. The laser sources, the beam splitter and the ABD telescope arranged geometrically in such a way that after passing the beam splitter, the combined beams are directed to the secondary mirror where they are reflected to the primary mirror and then further reflected towards the targeted object. In the case of a tiled fiber array as a source of the beam λ_{il}, the pocket array geometry matches the fiber-collimator array, so that each beamlet of the tiled fiber array sub-aperture enters the corresponding pocket region of the pocket-mirror and is then reflected from the pocket window. We note that there exists a modified version of the ABD system working with a single laser beam λ_{il}. In

this case the wavefront controlling elements are located within the primary mirror pockets, whereas the photo-elements needed to determine the value of the metric are situated separately.

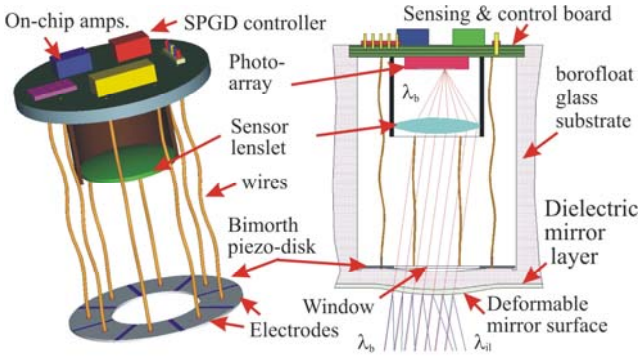

Fig.2. Schematics for wavefront control and sensing pocket of the ABD telescope primary mirror.

2.2. Function of the ABD system

As mentioned earlier, the ABD control system operates in a target-in-the-loop configuration. In this configuration the laser beam is sent through a disturbing media (atmospheric turbulence) towards a targeted object where it is scattered back and received by a detector. The detector signal is then used to close the control loop, serving as the input for a beam forming adaptive optics. The goal is to reduce the influence of the disturbing media and optimize the beam quality (hot-spot size) on the illuminated object.

In the described ABD system two laser beams with wavelengths λ_b and λ_{il} are leaving the ABD telescope and then are directed towards the targeted object through the turbulent air, which distorts the wavefront of both beams in the same way (see Fig.1). The laser beam with wavelength λ_b produces a beacon on the laser-illuminated object. Radiation from both beams is reflected back from the object towards the pocket mirror of ABD telescope but only the reflected radiation from the beacon beam λ_b can enter through the dielectric layer into the pockets whereas the scattered radiation from second beam is completely reflected. The back scattered light from the beacon beam λ_b is therefore detected by the photo-sensitive elements within the pockets and used for computing an input for the control algorithm which steers the wavefront correcting elements. This means that the adaptive elements primarily are correcting the turbulence induced wavefront aberration of the beacon beam. Since the difference in the wavelengths between the two used laser beams is only small which avoids wavelength anisoplanatism, the optimization of the spot size on the illuminated object for the laser beam with wavelength λ_b automatically also reduced the influence of the turbulent air and thus also optimizes the spot size for the laser beam with wavelength λ_{il}. By using two separate beams and a dielectric layer which blocks the transmission of illuminator beam into the pockets, it is possible to use on-mirror sensing of back scattered light within the beam path without the danger of too powerful illuminator beam disturbing the sensing of the back scattered light from the illuminated object or influence the functional elements within the pockets in an other unwanted way, e.g. by causing strong temperature gradients.

Sensing of the wave returned from the illuminated object is performed inside each pocket either by a single photo-detector or by a photo-detector array. The signals from these detectors are used to determine the metric values J which act as a quality parameter containing information about laser beam intensity concentration on the illuminated object. This metric is used as the input for the control algorithm.

Wavefront control in this system can be performed using the stochastic parallel gradient descent (SPGD) techniques [1,2]. Using metric values as the input, the SPGD algorithm computes iteratively new settings for the control voltages applied to the electrodes of the piezo-elements. Since the voltages of the piezo-elements control the curvature of the pocket-window front surface, this provides a compensation of low-order aberrations at each ABD pocket-window. If a phase-locked tiled fiber array is used as a source of the input for the illuminating beam of the ABD system, the pocket mirror provides higher order wavefront corrections beyond piston-control for each beamlet.

Besides strongly reducing the number of fiber-tiles necessary to correct the turbulence-induced wavefront aberrations, this also offers the opportunity to correct a possible misalignment of the fiber-tiles in the phase-locked tiled fiber array, thus making the whole system more robust. If otherwise a solid state laser is used as a source, the pocket mirror of the ABD system is the only adaptive beam forming element within the whole system which provides the capability to optimize the beam on the illuminated object.

3. Temporal speckle field analysis

3.1. Time-varying speckle metrics and time averaged power-in-the-bucket metrics

In this section we discuss in more detail different types of metrics required for adaptive laser beam control. The type of the used metric depends on the application. Power-in-the-bucket (PIB) metrics, averaging the total scattered radiation from the illuminated object received by photo-detectors, are useful in the case of point-source objects or as long as the beam size is larger than the illuminated object. A reduction of the beam size results in this case in a higher concentration of the laser energy on the object. This again leads to a higher intensity of the scattered radiation received by a detector. However, for the case of extended objects, that is when the intensity distribution of the laser beam completely falls within the outlines of the object, these metrics are problematical. In this case the power-in-the-bucket metrics perform poorly or not at all, depending on the curvature of the surface. Therefore an alternative metric is needed for extended objects.

Possible candidates for extended object metrics are time-varying speckle metrics. These are based on the observation that the signal of a single photo-detector shows fluctuations if the detector is placed in the speckle field reflected from the object and if the incident laser beam and object are moving relative to each other. Important is that the strength of these fluctuations and hence the power spectrum of the signal are dependent on the hot-spot size on the object. The smaller the hot-spot size the bigger the fluctuations and also the higher the frequency components which are present in the power spectrum.

In the ABD system, the following scenarios can be considered: (a) unresolved object; (b) extended fast spinning speckle-object; and (c) extended moving speckle-object with slow spin or none at all. Depending on the scenario the following methods for determining local and global metrics can be used:

- Distributed power-in-the-bucket metric for sensor unresolved objects. Photo-detectors, placed in lenslet focal planes, allow measurement of the power-in-the-bucket (PIB) metric $J_{PIB} = \sum_{j=1}^{N_p} J_j^{PIB}$, where Np is the number of pockets and J_j^{PIB} is the contribution to the PIB metric from the j-th pocket. Maximization of J_{PIB} leads to a compensation of phase aberrations and correspondingly increases the object hot-spot brightness.
- Distributed parallel time-varying speckle metric for extended objects. This type of metric is based on measurements of temporal and/or spatial correlation characteristics of the speckle field resulting from scattering off an extended object surface (speckle metrics J_s) [3,4]. Adaptive optics optimization of the speckle-metric allows mitigation of atmospheric effects for extended speckle-objects [3,5]. This processing of the returned wave requires a single photo-detector located in the pocket-lenslet focal plane. To separate different frequency components of the signal, signal processing includes spectral analysis of photo-current fluctuations.

Since the above described ABD system has the capability to work with resolved objects it is necessary to investigate the behavior of time-varying speckle metrics more closely. The relative to the object movement of the incident laser

beam needed for time-varying speckle metrics can be achieved in two ways. Either the object itself is moving or the laser beam is scanning over the surface of a stationary object. Therefore two types of experimental setups – one with a spinning object and another with a scanning beam – are used to investigate the time-varying speckle metrics [6].

3.2. Spinning object

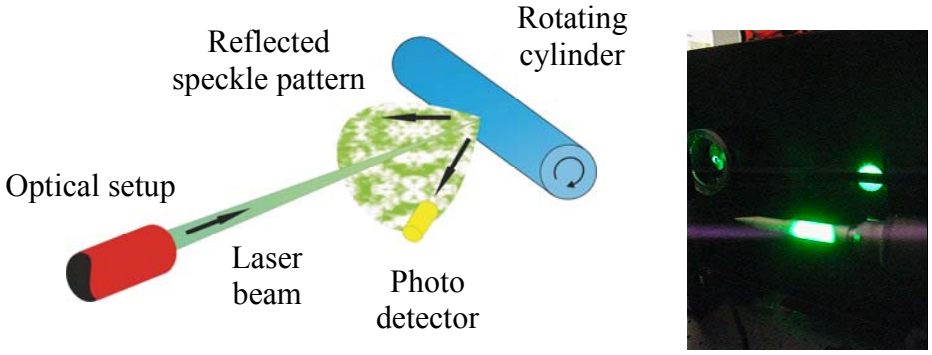

Fig.3. A schematic (left) and a photo (right) of the experimental setup for speckle experiments with a spinning object.

Fig.3 represents the experimental setup used for the time-varying speckle metrics behavior evaluation for the case of moving (spinning) objects. In this setup a laser beam with a wavelength of 532nm is cleaned with a micro-optic pinhole combination and collimated by a collimator lens with a focal length of 1m. A diaphragm is used to limit the beam size after collimation to 50mm. A second lens with a focal length of 300mm is mounted on a moveable stage and focuses the laser beam. After the lens a rotation symmetric object with a diameter of 14mm and a rough surface is placed within the laser beam in such a way that the axis of rotation of the object is perpendicular to the optical axis. The object is mounted on a drill with a rotation speed of 12rpm. By moving the position of the focusing lens, the position of the focal point relative to the object surface can be moved within a range of ±180mm. By increasing the distance of the focal point from the surface, the hot-spot size on the object can be controlled up to a diameter of 30mm. The minimum hot-spot size is 15µm. A photo-detector is placed in the reflected speckle pattern at a 50mm-distance from the object surface. The detector signal is digitized and read into a computer by a digital acquisition board.

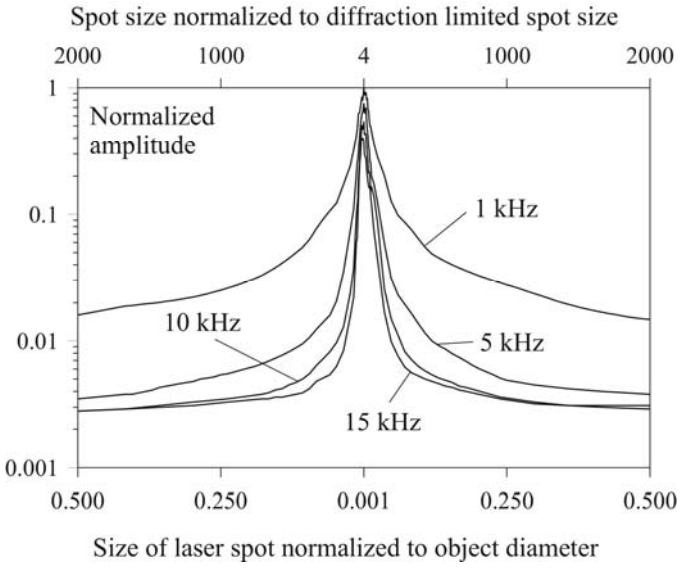

Fig.4. Dependence of the normalized amplitudes of several frequency components on the spot size on the object.

To use the speckle metrics as a quality parameter for laser beam intensity concentration, it is important to know the

dependence of the frequency component amplitudes on the laser hot-spot size. Fig.4. shows this dependence for four selected frequency components (1kHz, 5kHz, 10kHz, 15kHz), each with a bandwidth of 1kHz on the position of the focal point, and hence on the spot size on the object as measured with the described experimental setup. As seen, all frequency components have their maximum at the same position for the smallest hot-spot size. In addition, the width of the peaks for higher frequencies is smaller than the width for smaller frequencies.

Fig.5 shows the behaviors of the time-averaging metric $\langle J_{PIB} \rangle$, the time-varying metric J_s, and the combined metric J_Σ in dependence on the hot-spot size normalized to a spinning cylindrically shaped object. Here J_s is a weighted sum of the frequency components shown in Fig.4. The weights are chosen in such a way that for a smallest hot-spot size every frequency contributes equal to J_s. As seen from the Fig5, in the vicinity of small hot-spot sizes, the time-averaging metric $\langle J_{PIB} \rangle$ shows only weak sensitivity, whereas the time-varying metric J_s demonstrates rather high sensitivity. This leads to the conclusion that the time-varying speckle metrics are in particular useful for the optimization of the hot-spot size toward the possible limits. Fig.5 also shows that the combined metric J_Σ is advantageous before the single metrics J_s and $\langle J_{PIB} \rangle$. Although the time-varying metric J_s and also the combined metric J_Σ have a larger estimation error for small hot-spot sizes compared to the time averaging metric $\langle J_{PIB} \rangle$ – as is shown in the insets in Fig.5 – the range within which the hot-spot size can be confined due to estimation error is much smaller for the time-varying metric and the combined metrics. Whereas the combined metric J_Σ confines the hot-spot size within a diameter of 60µm, the time-averaging metric only determines the hot-spot size within a 1.3mm-range. The energy density within the hot spot can in this case be enlarged by a factor of (1.3mm/ 60µm ≈ 470) using the combined metric. Note that for other shapes of the illuminated object the time averaging metric might perform even worse for small hot-spot sizes. E.g. for objects with a uniform flat surface the time averaging metric is not sensitive to the spot size at all if the size of the hot spot is already smaller than the object size and if the intensity distribution falls completely within the outlines of the objects. According to the Lamberts cosine law which per definition holds for a diffuse reflecting Lambertian surface, the time-averaged power-in-the-bucket metric shows a dependency on the hot-spot size only for a curved surface.

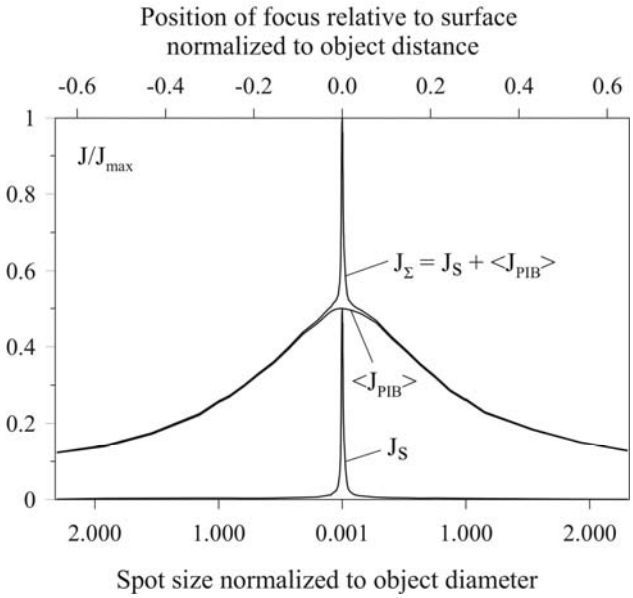

Fig.5. Dependence of the time-averaging metric $\langle J_{PIB} \rangle$, the time-varying metric J_s, and the combined metric J_Σ on the hot-spot size normalized to a spinning cylindrically shaped object. The insets are the zoomed maximum regions of the metrics $\langle J_{PIB} \rangle$ and J_Σ together with the standard error. The shaded area shows the accuracy with which the position of the maximum value, and therefore the hot-spot size, can be determined with each metric.

In addition to the possibility for a better final energy density the steeper gradient should also result in a faster convergence speed towards final optimization for the control algorithm of an adaptive optics. This is important if gradient based control algorithm like SPGD.

3.3. Scanning laser beam

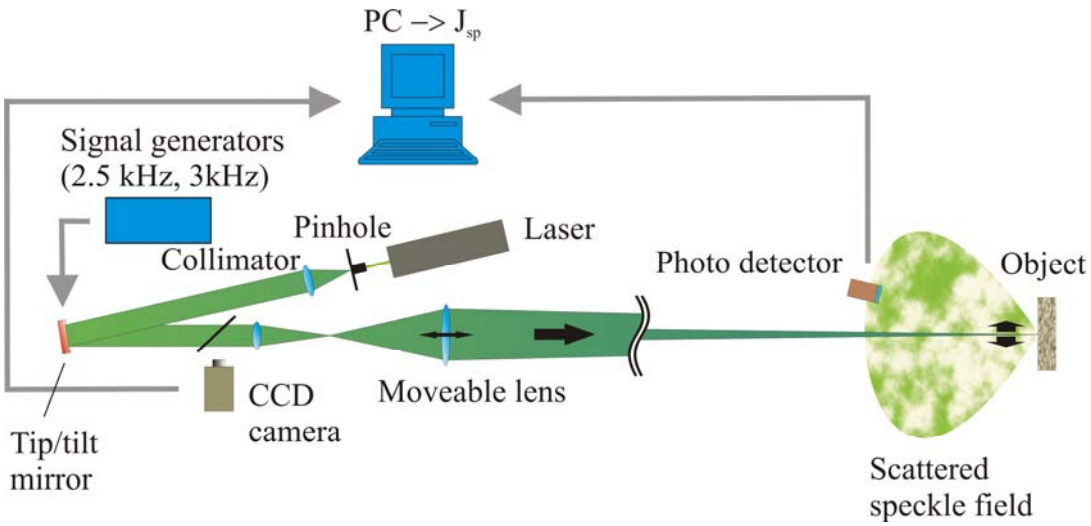

Fig.6. A schematic of the experimental setup for speckle experiments with a scanning laser beam.

To investigate the use of speckle metrics for non-moving (stationary) objects by means of a scanning laser beam an experimental setup is used containing a tip-tilt mirror to scan the laser beam over the surface of the object. The basic setup is shown Fig.6. A laser beam is cleaned with a micro-optic pinhole combination and collimated to a size of 13mm. The beam is then reflected by a tip-tilt mirror with a diameter of 14mm towards a relay-lens combination to increase the beam size to 50mm and focus it on the object at a distance of 8.25m. A beam splitter is placed between the tip-tilt mirror and the first relay lens, making it possible to image the illuminated object on the focal plane array of a CCD camera. One pixel of the camera covers a square of about 0.3×0.3mm on the object. The tip-tilt mirror is connected to two signal generators which are set to 3kHz (horizontal) and 2.5kHz (vertical). Since the relative speed between the object and the laser beam is much higher in this setup than in the non-scanning experimental setup described above higher frequencies (5kHz, 50kHz, 100kHz, 150kHz) with a bandwidth of 10kHz are chosen to determine the time-varying speckle metric J_s.

One important question for the scanning case is how the scanning amplitude influences the behavior of the speckle metric. The measured dependence of speckle metrics on the hot-spot size b_s for three different scanning amplitudes is shown in Fig.7. The insets show the images of the laser on the object (smallest hot-spot size $b_s^{\min}$) for a) no scanning, b) scanning with an amplitude of one times the minimum hot-spot size $b_s^{\min}$, c) scanning with an amplitude of two times the minimum spot size $b_s^{\min}$, and d) scanning with an amplitude of three times the minimum spot size $b_s^{\min}$. As seen from the figure, the maximum of all curves in Fig.7 are one the same position corresponding to the minimum hot-spot size $b_s^{\min}$. The width and shape of the curves are the same for all scanning amplitudes. Only the magnitude of the metric J_s is changing for different scanning amplitudes.

4. Conclusion

The ABD system has several advantages compared to conventional tiled fiber arrays used for laser beam control. Firstly, there is a dramatic reduction of system complexity and improvement of robustness against environmental influences which is offered by the direct integration of various beam control systems directly on the primary mirror. Secondly, the system has a wide range of potential applications since this concept of beam control works with unresolved and extended spinning and/or fast moving objects in the conditions of strong speckle modulation and intensity scintillations. Finally, the beam control approach discussed in this paper allows fast and high resolution return-wave sensing achieved with multiple photo-sensors and control hardware operating in parallel.

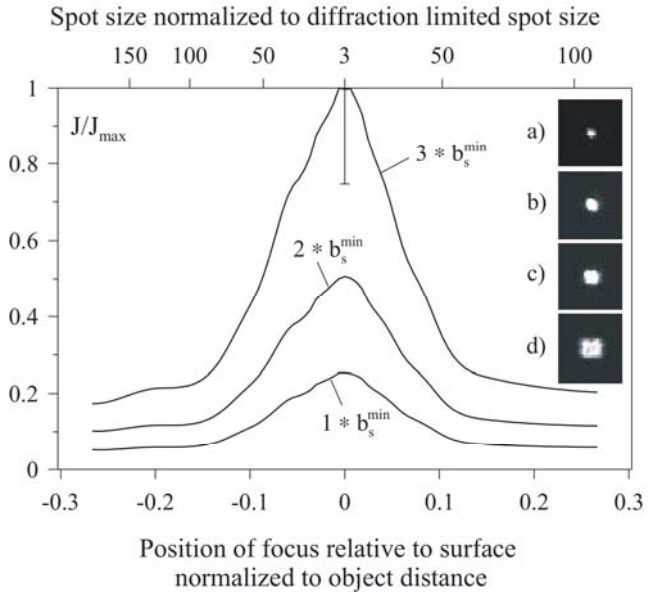

Fig.7. The dependence of speckle metrics on hot-spot size for three different scanning amplitudes is shown. The insets show the images of the laser on the illuminated object (smallest hot-spot size $b_s^{\min}$) for a) no scanning, b) scanning with an amplitude of one times the spot size $b_s^{\min}$, c) scanning with an amplitude of two times the spot size $b_s^{\min}$, and d) scanning with an amplitude of three times the spot size $b_s^{\min}$.

Our experiments show that time-varying speckle metrics can be used as metrics containing the information about the spot size on the illuminated extended objects. Due to strong sensitivity of these metrics for small laser spot sizes, they can increase the convergence speed of gradient based control algorithms, such as SPGD algorithms, and are in particular useful for the optimization of the laser spot towards the possible optimum. Moreover, a combination of the time-varying speckle metrics and the power-in-the-bucket metrics results in a universal metric which can be used for both the unresolved as well as for resolved objects.

5. REFERENCES

1. Weyrauch T., Vorontsov M., Beresnev L., and Liu L., Atmospheric compensation over a 2.3 km propagation path with a multi-conjugate (piston-MEMS/modal DM) adaptive system, Proc. SPIE, Vol. 5552, 73-84, 2004.
2. Vorontsov, M. A., Carhart G. W., Cohen M. and Cauwenberghs G., Adaptive optics based on analog parallel stochastic optimization: analysis and experimental demonstration, JOSA A, Vol. 17, 1440-1453, 2000.
3. Vorontsov M.A. and Carhart G., Adaptive phase distortion correction in strong speckle-modulation conditions, Optics Letters, Vol. 27, 2155-2157, 2002.
4. Polejaev V.I. and Vorontsov M.A., Adaptive active imaging system based on radiation focusing for extended target, SPIE, Vol. 3126, 216-220, 1997.
5. Vorontsov M.A. and Kolosov V., Target-in-the-loop beam control: basic considerations for analysis and wavefront sensing, JOSA A, Vol. 22, 126-141, 2005.
6. Polnau E., Vorontsov M.A., Beam Quality Metrics Based on Temporal Speckle Field Analysis in Directed Energy Applications for Extended Targets. JOSA A to be published, 2006